

## SOLUTION AIMING THE TECHNOLOGICAL IMPROVEMENT OF WORM AND STAR WHEEL FROM SINGLE SCREW COMPRESSOR

Gabriel FRUMUȘANU<sup>1,\*</sup>, Virgil TEODOR<sup>2</sup>, Nicolae OANCEA<sup>3</sup>

<sup>1), 3)</sup> Prof., PhD, Manufacturing Engineering Department, "Dunărea de Jos" University of Galați, Romania

<sup>2)</sup> Assoc. Prof., PhD, Manufacturing Engineering Department, "Dunărea de Jos" University of Galați, Romania

**Abstract:** *Single screw compressors are frequently used due to their constructive simplicity, leading to a lower price. The level of functional noise is also lower than in the case of other compressors. They usually include a central worm whose profile is generated by a star wheel with rectangular transversal profile. This paper proposes a solution enabling an easier machining of the worm, with the help of an end mill cutter. A new shape of the star wheel tooth is proposed, issuing from the analysis of central worm – star wheel gear, on the base of the fundamental theorems of reciprocal enwrapped surfaces. As consequence, a new constructive solution for the star wheel, which is the element that ensures compressor's sealing, is suggested. An analytical solution of the specific enwrapping surfaces problem is presented together with the new constructive shape of the star wheel.*

**Key words:** *single screw compressor, technological solution, worm profile, end mill cutter, new star wheel profile.*

### 1. INTRODUCTION

The Zimmern single screw compressor [1] has been invented in 1960. It is composed from a single helical worm (the main rotor) gearing in with two star wheels (the gate rotors), having their teeth in envelopment with worm axial section. The teeth play the role of sealing elements for the admission cavities of compressed agent. The worm has, usually, 6 threads, while the star wheels have 11 teeth each. In the case of higher working pressures, worms with 4 threads are used. Zimmern compressor can also work with liquid injection at 15-45 psi pressure, achieved by an auxiliary pump. Unlike Lysholm compressor, Zimmern compressor is cheaper and shows a lower level of noise in duty.

A new solution concerning the gate rotor tips profile and a dedicated manufacturing technology for the main rotor, performed on a 5-axis CNC milling machine were proposed [2]. The new build enables lower manufacturing cost, on common CNC machine tools.

After studying the surface of contact between gate rotor tooth and main rotor tooth, in order to improve the lubrication between the conjugated flanks for increasing compressor endurance, in [3] is presented a new type of tooth profile – a newly designed tooth flank of the meshing pair. Proposed flank surface of the gate rotor tooth has continuously varying curvature, which enables to obtain better conditions of lubrication during the relative motion respect the main rotor flank. The groove

flank is the envelop surface corresponding to the curved surface of the tooth flank. A specific mathematical model is also presented.

In this paper, a new manner to generate the flanks of compressor main rotor is proposed, together with a new build of the star wheels and a new profile for their teeth. The central worm – star wheel gear is analyzed on the base of fundamental theorems concerning the reciprocal enwrapped surfaces, and starting from here, the new shape of star wheel tooth, reciprocal enwrapped to central worm flank, is obtained.

Regarding paper structure, the next section presents the new shape of star wheel generating tooth. The third section is dedicated to finding the curve of contact between the conjugated flanks of central worm and star wheel. The fourth one presents a numerical application; the fifth proposes the new constructive solution for the star wheel, while the last section is for conclusion.

### 2. NEW SHAPE OF STAR WHEEL GENERATING TOOTH

The new shape of star wheel generating tooth is proposed to be a conical surface, materialized as a cylindro-conical shape attached to the circle of  $R$  radius, which is tangent to central worm cylinder of  $r$  radius (see Fig. 1). The worm flanks surfaces are generated through the following motions:

I – star wheel rotation of  $\varphi_1$  angular parameter;

II – central worm rotation of  $\varphi_2$  angular parameter;

III – cutting motion of cylindro-conical tool;

IV – indexing motion of the star wheel, needed for tool repositioning in order to generate the next groove (two successive positions are depicted in Fig. 1);

V – indexing motion of the central worm, necessary for repositioning a new groove.

\* Corresponding author: Domnească str. 111, RO-800201, Galați, Romania;  
Tel.: 0236/130208;  
Fax: 0236/314463;  
E-mail addresses: [gabriel.frumusanu@ugal.ro](mailto:gabriel.frumusanu@ugal.ro) (G. Frumușanu),  
[virgil.teodor@ugal.ro](mailto:virgil.teodor@ugal.ro) (V. Teodor),  
[nicolae.oancea@ugal.ro](mailto:nicolae.oancea@ugal.ro) (N. Oancea).



It should be noticed that in relations (7) the  $\varphi_2$  parameter does not appear because of its kinematical connection with  $\varphi_1$ :

$$\varphi_2 = i \cdot \varphi_1, \quad (8)$$

where  $i$  means the transmission ratio. More specific, if the central worm has  $k_r$  threads and the star wheel –  $z_t$  teeth, then relation (8) becomes:

$$\varphi_2 = \frac{z_t}{k_r} \cdot \varphi_1. \quad (9)$$

Usually,  $i = 11/6$ , [1].

### 3.3. The characteristic curve

The specific expression of the enveloping condition can be found [5, 6] starting from:

$$\begin{vmatrix} \dot{\xi}_\theta & \dot{\eta}_\theta & \dot{\zeta}_\theta \\ \dot{\xi}_u & \dot{\eta}_u & \dot{\zeta}_u \\ \dot{\xi}_{\varphi_1} & \dot{\eta}_{\varphi_1} & \dot{\zeta}_{\varphi_1} \end{vmatrix} = 0. \quad (10)$$

The elements of the determinant from left side of relation (10) are the partial derivatives of  $\xi$ ,  $\eta$  and  $\zeta$  coordinates from (6) against variables  $\theta$ ,  $u$  and  $\varphi_1$ :

$$\begin{cases} \dot{\xi}_\theta = B \sin \theta \sin \varphi_1 \cos \varphi_2 - B \cos \theta \sin \varphi_2; \\ \dot{\eta}_\theta = -B \sin \theta \cos \varphi_1; \\ \dot{\zeta}_\theta = B \sin \theta \sin \varphi_1 \sin \varphi_2 + B \cos \theta \cos \varphi_2, \end{cases} \quad (11)$$

$$\begin{cases} \dot{\xi}_u = (-\cos \varphi_1 + \tan \alpha) \cos \varphi_2 + \tan \alpha \sin \theta \sin \varphi_2; \\ \dot{\eta}_u = -\sin \varphi_1 - \tan \alpha \cos \theta \cos \varphi_1; \\ \dot{\zeta}_u = (-\cos \varphi_1 + \tan \alpha) \sin \varphi_2 - \tan \alpha \sin \theta \cos \varphi_2, \end{cases} \quad (12)$$

$$\begin{cases} \dot{\xi}_{\varphi_1} = (u \sin \varphi_1 - B \cos \theta \cos \varphi_1) \cos \varphi_2 - \\ - i \cdot \sin \varphi_2 (-u \cos \varphi_1 - B \cos \theta \sin \varphi_1 + R + r) - \\ - B \cdot i \cdot \sin \theta \cos \varphi_2; \\ \dot{\eta}_{\varphi_1} = -u \cos \varphi_1 - B \cos \theta \sin \varphi_1; \\ \dot{\zeta}_{\varphi_1} = (u \sin \varphi_1 - B \cos \theta \cos \varphi_1) \sin \varphi_2 + \\ + i \cdot \cos \varphi_2 (-u \cos \varphi_1 - B \cos \theta \sin \varphi_1 + R + r) - \\ - B \cdot i \sin \theta \sin \varphi_2. \end{cases} \quad (13)$$

The ensemble of equations (6), relation (9), condition (10) and relation (11) – (13), for a given value of  $\varphi_1$ , represent the curve of contact between the central worm flank and the cylindro conical surface (2),  $C_S$ . When  $\varphi_1 = 0$ , the enveloping condition (used in order to find the characteristic curve) becomes:

$$\begin{vmatrix} 0 & -\sin \theta & \cos \theta \\ \tan \alpha - 1 & -\tan \alpha \cos \theta & -\tan \alpha \sin \theta \\ -B(\cos \theta + i \sin \theta) & -u & i(R + r - u) \end{vmatrix} = 0. \quad (14)$$

Hence, the contact line on surface  $S$ , meaning the sealing line of space  $S$  – the central worm flank is

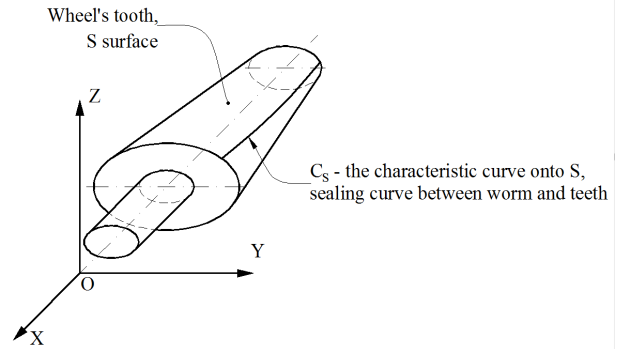


Fig. 3. The characteristic curve.

determined through the ensemble of equations (2) of surface  $S$ , the enveloping condition (14) and the condition  $\varphi_1 = 0$  (leading also to  $\varphi_2 = 0$ ).

### 3.4. Flank surface of the central worm groove

The flank surface of the central worm groove can be determined by giving to  $C_S$  curve the motion (3), in this case the matrix  $X$  meaning the locus of the points belonging to  $C_S$ .

## 4. NUMERICAL APPLICATION

The shape of the characteristic curve  $C_S$  (the sealing line between the central worm flank and the star wheel tooth) is further studied in numerical form, with the help of a dedicated MatLab application. The input data are the values of the parameters defining the gear geometry (see Fig. 2 and 3), namely:

- $R$ , meaning the radius of the star wheel centrede;
- $r$  – the distance between central worm centrede and its symmetry axis;
- $R_i$  – the star wheel foot radius;
- $a$  – the height of star wheel tooth head;
- $b$  – half of the star wheel tooth width, measured at his head;
- $\alpha$  – the angle of tooth flank inclination;
- $i$  – the transmission ratio (see (8) and (9)).

The algorithm after which the application below presented works supposes the following steps:

- $u$  parameter is discretized in  $n_u$  points between  $u_{min}$  and  $u_{max}$  (see 3.1 section);
- for each value of  $u$ ,  $\theta$  parameter is also discretized in  $n_\theta$  points between 0 and  $\pi$ ;
- the absolute value of the determinant from (14) is calculated for each couple  $(u, \theta)$  and if it is smaller than the maximum admissible error for numerically solving the equation (14) –  $\varepsilon$ , then the coordinates of the corresponding point belonging to  $C_S$  are calculated (relative to  $XYZ$  system) with (2).

The application has been run for the set of geometrical parameters values defining an actual gear, namely:  $R = 45$  mm,  $r = 30$  mm,  $R_i = 40$  mm,  $a = 5$  mm,  $b = 5$  mm,  $\alpha = 20^\circ$ ,  $i = 11/6$ . The values of the auxiliary variables has been chosen as  $n_u = 101$ ,  $n_\theta = 5001$ ,  $\varepsilon = 0.1$ . The results delivered in this case are sampled in Table 1, the characteristic curve  $C_S$  profile is depicted in Fig. 4, and its positioning on tool surface is shown in Fig. 5.

```

% Central worm - star wheel gear (modified profile)
R=45; Ri=40; b=5; a=5; r=30;
alfa=pi/9; eps=0.1;
umin=Ri; umax=R+a;
f1=0;
i=11/6; f2=i*f1;
k=1;
for u=umin:0.1:umax;
    foundpoint=0;
    B=b+(R+a-u)*tan(alfa);
    for t=0:0.0002:pi;
        if (foundpoint==0)
            X=-u;
            Y=B*cos(t);
            Z=B*sin(t);
            csi=cos(f2)*(X*cos(f1)-Y*sin(f1)+R+r)-sin(f2)*Z;
            eta=X*sin(f1)+Y*cos(f1);
            zeta=sin(f2)*(X*cos(f1)-Y*sin(f1)+R+r)+cos(f2)*Z;
            M(1,1)=(-cos(f1)+tan(alfa))*cos(f2)+tan(alfa)*sin(t)*sin(f2);
            M(1,2)=-sin(f1)-tan(alfa)*cos(t)*cos(f1);
            M(1,3)=(-cos(f1)+tan(alfa))*sin(f2)-tan(alfa)*sin(t)*cos(f2);
            M(2,1)=(u*sin(f1)-B*cos(t)*cos(f1))*cos(f2)-i*(-u*cos(f1)-
                -B*cos(t)*sin(f1)+R+r)*sin(f2)-i*B*sin(t)*cos(f2);
            M(2,2)=-u*cos(f1)-B*cos(t)*sin(f1);
            M(2,3)=(u*sin(f1)-B*cos(t)*cos(f1))*sin(f2)+i*(-u*cos(f1)-
                -B*cos(t)*sin(f1)+R+r)*cos(f2)-i*B*sin(t)*sin(f2);
            M(3,1)=B*sin(t)*sin(f1)*cos(f2)-B*cos(t)*sin(f2);
            M(3,2)=-B*sin(t)*cos(f1);
            M(3,3)=B*sin(t)*sin(f1)*sin(f2)+B*cos(t)*cos(f2);
            d=det(M);
            if (abs(d)<eps)
                tt(k,1)=t;
                uu(k,1)=u;
                Xc(k,1)=csi;
                Yc(k,1)=eta;
                Zc(k,1)=zeta;
                Xc0(k,1)=X;
                Yc0(k,1)=Y;
                Zc0(k,1)=Z;
                foundpoint=1;
                k=k+1;
            end;
        end;
    end;
end;
end;
end;

```

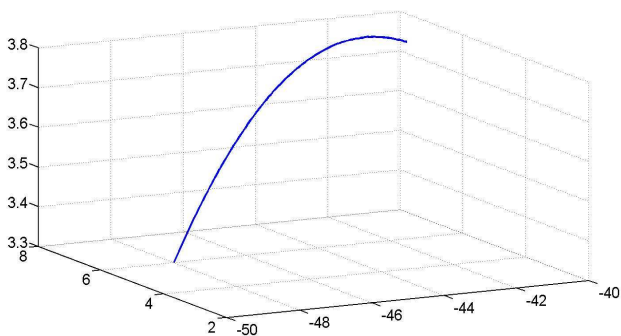


Fig. 4. The characteristic curve shape.

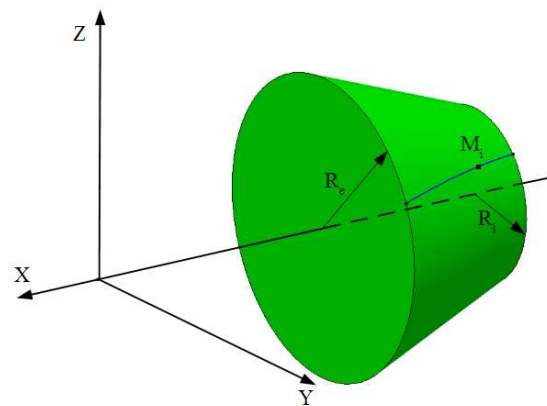


Fig. 5. Characteristic curve positioning onto cylindro-conical tool surface.

Table 1

Coordinates of characteristic curve points

Point crt. no.	$u$ [mm]	$\theta$ [rad]	$X$ [mm]	$Y$ [mm]	$Z$ [mm]
1	40	0.4464	-40	7.793	3.730
2	40.100	0.4488	-40.100	7.751	3.733
3	40.200	0.4514	-40.200	7.708	3.737
4	40.300	0.4540	-40.300	7.666	3.741
5	40.400	0.4564	-40.400	7.624	3.743
6	40.500	0.4590	-40.500	7.582	3.747
7	40.600	0.4616	-40.600	7.539	3.751
8	40.700	0.4642	-40.700	7.497	3.754
9	40.800	0.4668	-40.800	7.455	3.757
10	40.900	0.4694	-40.900	7.413	3.760
11	41	0.4720	-41	7.370	3.763
12	41.100	0.4746	-41.100	7.328	3.765
13	41.200	0.4772	-41.200	7.286	3.767
14	41.300	0.4798	-41.300	7.244	3.770
15	41.400	0.4826	-41.400	7.201	3.773
.....					
41	44	0.5546	-44	6.107	3.783
42	44.100	0.5574	-44.100	6.065	3.780
43	44.200	0.5604	-44.200	6.023	3.779
44	44.300	0.5634	-44.300	5.981	3.778
45	44.400	0.5662	-44.400	5.939	3.775
46	44.500	0.5692	-44.500	5.897	3.773
47	44.600	0.5722	-44.600	5.855	3.771
48	44.700	0.5750	-44.700	5.814	3.768
49	44.800	0.5780	-44.800	5.772	3.765
50	44.900	0.5810	-44.900	5.731	3.763
51	45	0.5840	-45	5.689	3.760
52	45.100	0.5870	-45.100	5.647	3.757
53	45.200	0.5900	-45.200	5.606	3.753
54	45.300	0.5930	-45.300	5.564	3.750
55	45.400	0.5960	-45.400	5.523	3.746
.....					
87	48.600	0.6976	-48.600	4.222	3.539
88	48.700	0.7010	-48.700	4.182	3.530
89	48.800	0.7044	-48.800	4.142	3.520
90	48.900	0.7076	-48.900	4.103	3.510
91	49	0.7110	-49	4.064	3.500
92	49.100	0.7144	-49.100	4.024	3.490
93	49.200	0.7178	-49.200	3.985	3.480
94	49.300	0.7212	-49.300	3.946	3.469
95	49.400	0.7244	-49.400	3.908	3.458
96	49.500	0.7278	-49.500	3.869	3.447
97	49.600	0.7312	-49.600	3.830	3.436
98	49.700	0.7346	-49.700	3.791	3.424
99	49.800	0.7380	-49.800	3.752	3.413
100	49.9000	0.7416	-49.9000	3.713	3.401
101	50	0.7450	-50	3.675	3.389

## 5. NEW CONSTRUCTIVE SOLUTION FOR THE STAR WHEEL

### 5.1. The proposed constructive solution

As it can be noticed from the above presented numerical simulation, the sealing line is an almost plane curve – the coordinates of its points along Z axis vary in an interval with length smaller than 0.5 mm. Therefore, it may be accepted that a sector of the cylindro-conical, thick enough to include  $C_s$  curve on its both flanks, can substitute the star wheel tooth (see Fig. 6).

A new constructive solution for the star wheel has been developed (Fig. 7) by starting from the new shape of the tooth. It has the unquestionable advantage of presenting an easier manufacturability of teeth. They can be machined separately, individually and afterwards assembled to wheel main body by using a thread practiced on tooth stem and a screw nut placed inside a dedicated groove. The possibility of tooth rotation is annulled with the help of a key. The conjugated worm in the case of using such a star wheel is obviously a globoid worm.

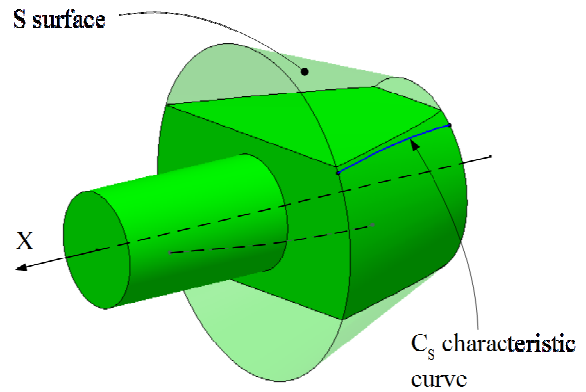


Fig. 6. The newly shaped star wheel tooth.

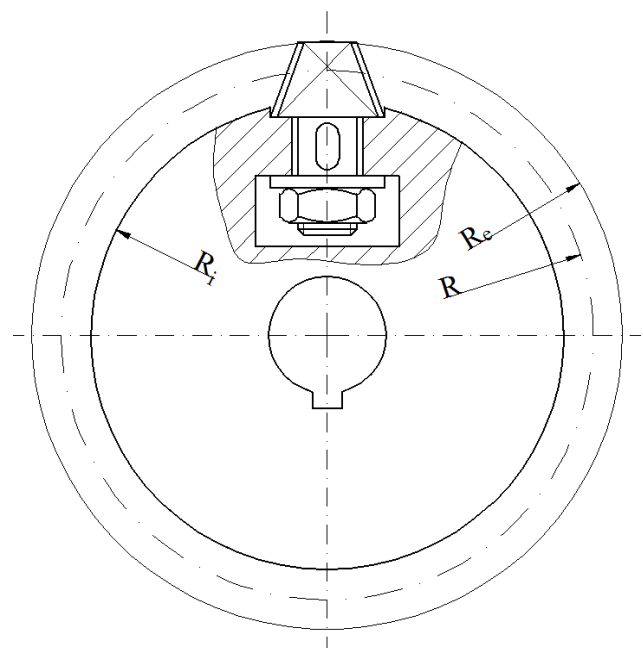


Fig. 7. The new type of star wheel.

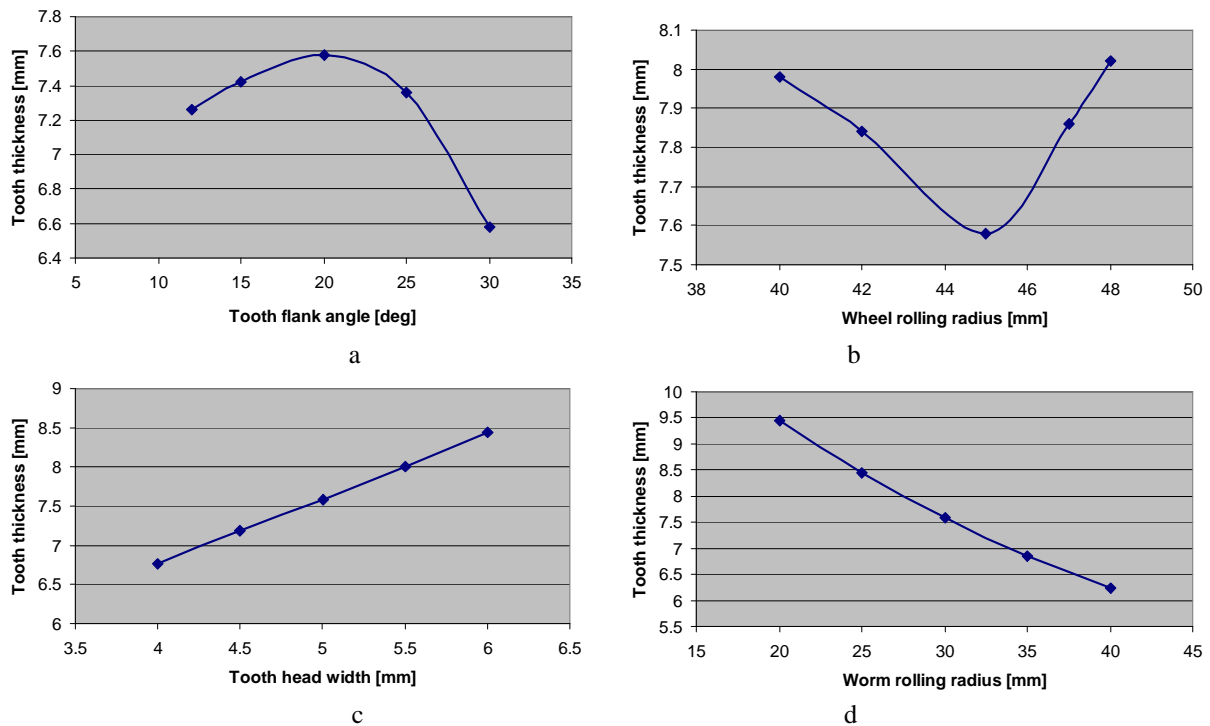


Fig. 8. Constructive parameters influence onto tooth thickness.

## 5.2. Star wheel tooth thickness

As it can be noticed from Fig. 6, the star wheel tooth is actually a "slice" from the cylindro-conical tool. Its thickness is determined by the position of the characteristic curve on tool surface – more specific, by  $Z$  coordinate of characteristic curve's points. Because tooth thickness has a significant impact on central worm – star wheel gearing quality, the influence of some of the more important parameters defining gearing geometry (tooth flank angle, wheel rolling radius, tooth head width, worm rolling radius) has been studied. Each one of the mentioned parameters has been varied separately, while the other ones have been kept unchanged, at the nominal values mentioned at the beginning of the fourth section.

The results are presented in graphical form in Fig. 8 and they are showing that gear design parameters have a noticeable impact onto tooth thickness, hence they should be carefully chosen.

## 6. CONCLUSIONS

The new constructive solution of star wheel for Zimmern compressors, having teeth formed by sectors of the cylindro-conical solid, despite being more complicated than the existing solution, has the advantage of enabling a better sealing of compressor working room along the contact line  $C_3$ .

Another significant advantage of the proposed solution is the possibility of machining the main rotor worm with a cylindro-conical tool on a CNC machine tool with five axis, both flanks of the worm groove resulting simultaneously.

Specialized equipment that can generate with a profiled end mill cutter the main rotor worm can also be further imagined.

## REFERENCES

- [1] B. Zimmern, G.C. Patel, *Design and Operating Characteristics of the Single Screw Compressors*, International Compressors Engineering Conference, Purdue e-Pubs, pp. 96–99, 1972, Purdue.
- [2] D. Jensen, *A New Single Screw Compressor Design that Enables a New Manufacturing Process*, International Compressors Engineering Conference, Purdue e-Pubs, pp. 601–604, 1998, Purdue.
- [3] J. Li, F. Liu, Q. Feng, W. Wu, *A New Design of the Tooth Profile for Single Screw Compressors*, International Compressors Engineering Conference, Purdue e-Pubs, pp. 1–6, 2012, Purdue.
- [4] F.L. Litvin, *Theory of gearing*, NASA, Scientific and Technical information Division, Washington DC, 1984.
- [5] S.P. Radzevich, *Kinematics Geometry of Surface Machining*, CRC Press, London, 2008.
- [6] N. Oancea, *Surfaces generation through winding, vol. I – III*, Galati University Press, Galați, 2004.